frontiers | Frontiers in Chemistry

TYPE Original Research
PUBLISHED 19 September 2023
DOI 10.3389/fchem.2023.1267634

OPEN ACCESS

EDITED BY
Diego Mauricio Gil,
Universidad Nacional de Tucumán, Argentina

REVIEWED BY
Antonio Carlos Sant'Ana,
Juiz de Fora Federal University, Brazil
Evangelia Tzanetou,
Benaki Phytopathological Institute, Greece

*CORRESPONDENCE
Antônio S. N. Aguiar,
toninho.quimica@gmail.com
Hamilton B. Napolitano,
hbnapolitano@gmail.com

RECEIVED 26 July 2023
ACCEPTED 07 September 2023
PUBLISHED 19 September 2023

CITATION
Aguiar ASN, Costa LB, Borges ID, Aguirre G, Tejerina-Garro FL, Dutra e Silva S and Napolitano HB (2023), The effect of water molecules on paraquat salts: from physicochemical properties to environmental impact in the Brazilian Cerrado.
Front. Chem. 11:1267634.
doi: 10.3389/fchem.2023.1267634

The effect of water molecules on paraquat salts: from physicochemical properties to environmental impact in the Brazilian Cerrado

Antônio S. N. Aguiar [1]*, Luiz B. Costa [2], Igor D. Borges [1,2], Gerardo Aguirre [3], Francisco L. Tejerina-Garro [2,4], Sandro Dutra e Silva [2] and Hamilton B. Napolitano [1,2]*

[1]Programa de Pós-Graduação em Recursos Naturais do Cerrado, Universidade Estadual de Goiás, Anápolis, Brazil, [2]Programa de Pós-Graduação em Sociedade, Tecnologia e Meio Ambiente, Universidade Evangélica de Goiás, Anápolis, Brazil, [3]Centro de Graduados e Investigación en Química, Tecnológico Nacional de Mexico, Tijuana, Mexico, [4]Escola de Ciências Médicas e da Vida, Pontifícia Universidade Católica de Goiás, Goiânia, Brazil

Introduction: The green revolution model that is followed in the Brazilian Cerrado is dependent on mechanization, chemical fertilization for soil dressing and correction, and the use of herbicides. Paraquat is a methyl viologen herbicide marketed as bipyridylium dichloride salts and used (in low doses) to combat weeds in their post-emergence stage. It is a non-selective pesticide that causes the peroxidation of the lipids that make up the cell membrane, and when it comes into contact with foliage, it results in the death of the plant.

Methods: The effect of water molecules co-crystallized in Paraquat salt structures was analyzed in anhydrous, dihydrate, and trihydrate forms to understand those physicochemical properties in its redox activity. The frontier molecular orbitals were also carried out using DFT to obtain the chemical reactivity of the bipyridylium cation. Finally, the supramolecular arrangements were evaluated to analyze the physicochemical stability and acquire insights on superoxide anions.

Results and discussion: The electronic structure indicated that the BP cation presents an acidic character due to its low ELUMO value, while the salt has a more basic character due to its high EHOMO value. For this reason, the BP ion is more susceptible to reduction during the weeds' photosynthesis process. During the process of plant photosynthesis, PQ is reduced to form a stable radical cation. In the supramolecular arrangement, the presence of water molecules increases the number of strong H-bonds, while the weak/moderate H-bonds are stabilized. PQ's toxic effects are observed in wildlife, domesticated animals, human populations, and ecosystems. The influence of PQ on the terrestrial environment is limited because of the soil adsorption capacity associated with good agricultural practices. The current use of good agricultural practices in the Cerrado seems not to prevent the environmental impacts of herbicides like PQ because it aims for the expansion and profitability of large-scale farming based on input-intensive practices instead of sustainable agriculture processes.

KEYWORDS
Paraquat, physicochemical properties, green revolution, Brazilian Cerrado, herbicide

1 Introduction

Paraquat (PQ) is a herbicide available in the *1,1'-dimethyl-4,4'-bipyridilium chloride* salt form. It is a methyl viologen compound first described in 1882, with redox properties discovered only in 1933 (Michaelis et al., 1933), and herbicidal properties described in 1958 (Brian et al., 1958). From then on, PQ began to be developed for commercial purposes, becoming available on the agricultural market in 1962. It is a non-selective, fast-acting contact herbicide used to control a broad spectrum of broadleaf weeds and grasses in sugarcane (Aekrathok et al., 2021), soybean (da Silva et al., 2021), cotton (Ferreira et al., 2018), rice (Lima et al., 2018), coffee (de Queiroz et al., 2018) and in fruit such as grapes, apples, and pineapples. PQ is listed under a pesticide category in regulatory classifications (*e.g.*, United States Environmental Protection Agency) due to its primary use.

As bipyridylium (BP) salt, PQ interrupts photosynthesis processes in plants, so that the main effect observed is the burning of plant tissue after exposure to light. This is because its mechanism of action consists of the electronic competition of the herbicide with photosystem I (PSI) ferredoxin present in chloroplasts during plant photosynthesis (Fukushima et al., 2002). PQ is reduced by NADPH-cytochrome *c* reductase, producing viologen methyl radicals that are instantly oxidized with O_2—forming the superoxide radical (O_2 $\cdot^-$), by cytochrome P-450 in the presence of tertiary amine N-oxides. In addition, other toxic oxygen species, including the hydroxyl radical (OH ·), hydrogen peroxide (HOO ·), and singlet oxygen ($^1O_2$), are formed, causing peroxidation of the lipids that constitute the cytoplasmic membrane, resulting in water loss and rapid desiccation of the plant, leading to its death (Dodge, 1982; Fukushima et al., 2002; Cui et al., 2019).

PQ is applied during the post-emergence stage of weeds (Cui et al., 2019). It is rapidly absorbed by the soil, undergoing a sorption process primarily driven by ion exchange, leading to deactivation (Weber and Weed, 1968). This herbicide can enter the aquatic environment via vertical transport through the soil profile (dissolved organic matter colloids and dispersal colloidal clay) (Santos et al., 2013) or runoff during the rainfall season (Veríssimo et al., 2018). This herbicide is highly soluble in water (561–700 g/L) (Tsai, 2013; Huang et al., 2019), but in waterbodies, it tends to be adsorbed by particles and sediment, displaying a half-life time between 2 and 820 years, depending on sunlight and water depth (Thi Hue et al., 2018). PQ has been found in surface and underground water, the former involving a potential source for drinking water contamination (Rial-Otero et al., 2006; Santos et al., 2013). In aqueous solutions, PQ can be photochemically degraded in the presence of oxygen and ultraviolet radiation (Tsai, 2013).

The Cerrado–*a neotropical savanna*–is the second largest Brazilian biome, encompassing originally about two million km^2 (Oliveira and Marquis, 2002). This biome has been used since the Brazilian green revolution, forming the main agricultural Frontier and becoming one of the global centers for the production of grains and commodities (Michaelis et al., 1933; Brian et al., 1958; Dutra e Silva, 2023). In Brazil, the technique of choice since 1980 had been no-till agriculture, accompanied by the use of herbicides, mainly PQ, until 2020, when its use was banned (Ofstehage and Nehring, 2021). The green revolution model followed in Brazil has been based on a pattern of mechanization, chemical fertilization for soil dressing and correction, in addition to the use of *pesticides* to control pests and insects. In recent years, the country has stood out as one of the main import markets for pesticides, many of which are banned in their own countries of origin, especially by the European Union (Cabette et al., 2020; Rocha et al., 2022a; Rocha et al., 2022b). The discussion on *control* and/or *flexibility* in the use of pesticides in Brazil is associated with the context of the green revolution in the country (Glaeser, 2010; Paumgartten, 2020).

PQ is an example of the controversies and struggles among those who are in favor of or against the greater release of pesticides in Brazilian agriculture (Brazil, 2020). This issue is still complex, and there is no consensus on the *risks* and *benefits* of using PQ in agricultural production (Brown et al., 2004; Shoham, 2013). Few studies have been conducted about the impacts of PQ on the Cerrado biome: Lajmanovich (Lajmanovich et al., 1998) concludes that the tadpole *Scinax nasica* present in Cerrado regions underwent increased mortality when exposed to 30.0 and 50.0 mg PQ/L. Peruzzolo (Peruzzolo et al., 2021) indicate that the ingestion of PQ increases the mortality of *Scaptotrigona bipunctata*, a native bee found in the Cerrado; Lundberg (Lundberg, 2021) considered the use of herbicides in soybean crops between 2016 and 2018 and points out that PQ displays a very high potential impact on freshwater species because of the high value of its ecotoxicity, as measured by chemical toxic unit (CTU per kg released). Finally, the Brazilian ban on PQ use was based on its mutagenic potential in human germ cells in contact with this herbicide.

In this work, the effects of water molecules on the crystalline structures of PQ salts were described. Theoretical calculations were carried out using density functional theory (DFT) (Hohenberg and Kohn, 1964; Kohn and Sham, 1965), where the cation molecular and electronic structures of BP were analyzed. The chemical reactivity descriptors were obtained from Frontier molecular orbitals (FMO) (Zhang and Musgrave, 2007) to understand the influence of Cl^-anions in the vicinity of the cation and simulate the effects on the cell environment. Furthermore, the physicochemical information on the capture of electrons during the herbicide's action in the photosynthetic processes of plants (Fukushima et al., 2002) was obtained based on the spin density (Overhauser, 1962; Jacob and Reiher, 2012). Finally, the supramolecular arrangements of the anhydrous, dihydrate, and trihydrate PQ salts were analyzed on a physicochemical basis and associated with environmental impact in the Brazilian Cerrado.

2 Methods

2.1 Molecular modeling

The crystal structures of the PQ salts (1,1'-dimethyl-4,4'-bipyridylium dichloride), in anhydrous (PQC-I) (Russell and Wallwork, 1972), dihydrate (PQC-II) (Cousson et al., 1993), and trihydrate (PQC-III) (Argay and Kálmán, 1995) forms were obtained from the Cambridge Crystallographic Data Centre (CCDC) (Cambridge Crystallographic Data Centre, 2023), under codes 1228234, 1170961, and 110220, respectively. The crystal

TABLE 1 Crystallographic data and structure refinement for PQC-I, PQC-II, and PQC-III.

Crystal data	PQC-I	PQC-II	PQC-III
Chemical formula	$C_{12}H_{14}N_2Cl_2$	$C_{12}H_{14}N_2Cl_2 \cdot 2H_2O$	$C_{12}H_{14}N_2Cl_2 \cdot 3H_2O$
Molecular weight (g/mol)	257.158	293.188	311.203
Space group	Pnma (Orthorhombic)	P $\bar{1}$ (Triclinic)	P $2_1/c$ (Monoclinic)
a (Å)	9.22 ± 0.01	9.696 (3)	9.061 (1)
b (Å)	10.76 ± 0.01	11.322 (4)	16.229 (3)
c (Å)	5.88 ± 0.01	7.076 (3)	11.322 (1)
α (°)	90	100.68 (4)	90
β (°)	90	93.40 (3)	108.68 (1)
γ (°)	90	107.04 (4)	90
V (Å^3)	1575.41	724.468	1577.21
Z	4	2	4

structure data of the salts is presented in Table 1, and the structural patterns were analyzed in the Mercury program (Macrae et al., 2006; Macrae et al., 2008). Theoretical calculations were carried out by DFT (Hohenberg and Kohn, 1964; Kohn and Sham, 1965), implemented in the Gaussian 16 program package (Frisch et al., 2016). For the calculations, the hybrid exchange-correlation functional with long-range correction, M06-2X (Zhao and Truhlar, 2008), combined with the basis set 6-311++G(d,p), in gas phase, was used. By the FMO energies (Zhang and Musgrave, 2007), the highest occupied molecular orbital (HOMO) and lowest unoccupied molecular orbital (LUMO), it was possible to compare the electronic structures of the BP cation and its respective salt, as well as to infer information about their chemical reactivity and kinetic stability. Spin density calculations (Overhauser, 1962; Jacob and Reiher, 2012) were also carried out to obtain information about the radical formed during the mechanism of action of the herbicide (Fukushima et al., 2002) on the photosystems of the weed.

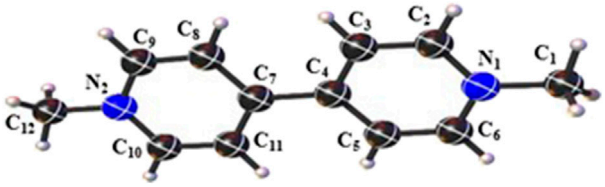

FIGURE 1
Solid-state *Ortep* representation of Paraquat, where the ellipsoids are drawn at the 50% probability level.

2.2 Supramolecular arrangement

The supramolecular arrangements of the respective PQ salts were studied by normalized Hirshfeld surfaces (HS) (Spackman and Jayatilaka, 2009) and 2D fingerprint plots (Spackman and McKinnon, 2002) using the program CrystalExplorer17 (Turner et al., 2017). Then, the topological parameters were obtained by the quantum theory of atoms in molecules (QTAIM) (Bader, 1985; Bader, 1994) using the Multiwfn program (Lu and Chen, 2012). In QTAIM, the observable properties of the molecular system are contained in the electron density $\rho(\mathbf{r})$ of the molecular topology. The Laplacian of the electron density, $\nabla^2\rho$, is a parameter that determines depletions and peaks of electron charge concentration between nuclear attractors in the molecular system topology, indicating the location of the bond critical points (BCP). In other words, $\nabla^2\rho$ indicates the concentration of electronic charge in the intranuclear region of two attractors: electronic density accumulated in the intranuclear region will result in a BCP with $\nabla^2\rho < 0$; electronic density accumulated in the attractors (depletion in the BCP) will result in a BCP with $\nabla^2\rho > 0$ (Bader, 1985; Matta and Bader, 2003). In the first case, the interaction is *shared*, such that the attractors are covalently bonded, while in the second case, the interaction is of the *closed-shell* type, in which the attractors are connected by weak electrostatic interactions (Bader, 1985; Bader, 1994). The topological parameters obtained by QTAIM are shown in Supplementary Table S1 (Supplementary Material S1). The results obtained low values of the electron density ($\rho <$ 0.1 au) and positive values of the Laplacian $\nabla^2\rho > 0$, indicating that the charge is depleted at the bond critical point (BCP). By the virial theorem,

$$\frac{1}{4}\nabla^2\rho(\mathbf{r}) = 2G(\mathbf{r}) + v(\mathbf{r}), \quad (1)$$

in atomic units, and by the expression,

$$h(\mathbf{r}) = G(\mathbf{r}) + v(\mathbf{r}), \quad (2)$$

it was shown that the energy topological parameters are related to $\nabla^2\rho$, where $h(\mathbf{r})$ corresponds to the electron density energy, $G(\mathbf{r})$ to the kinetic energy density, and $v(\mathbf{r})$ to the potential energy density. For H bonds, it was shown that the intensity of the interaction is very strong for $\nabla^2\rho < 0$ and $h < 0$ values, strong for $\nabla^2\rho > 0$ and $h < 0$ values, and weak or moderate for $\nabla^2\rho > 0$ and $h > 0$ values (Carroll and Bader, 1988). The binding energies (*BE*) (Emamian et al., 2019) were calculated using the formula,

$$BE \approx -332.34\rho(\mathbf{r}) - 1.0661, \quad (3)$$

where *BE* is given in kcal/mol.

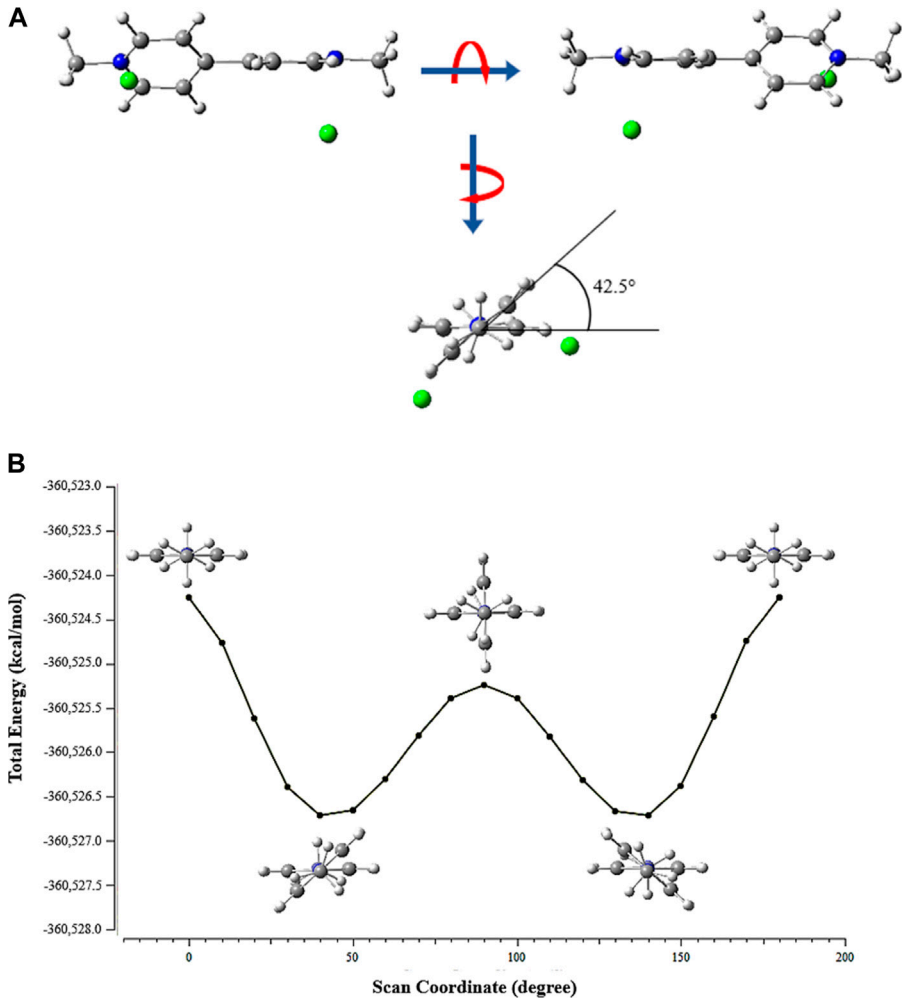

FIGURE 2
(A) The torsional effect on the bipyridylium cation structure by the presence of the Cl^- anions and **(B)** the relaxed scan of the energy due to the rotation of the C_4–C_7 bond by 180°.

3 Results and discussion

3.1 Molecular modeling analysis

PQ consists of a quaternary BP structure (Figure 1) formed by the connection of two pyridine rings. In this structure, the N atoms are diametrically apart and, bonded in the *para*-position, a methyl group is present on each aromatic ring. The compound is produced in the form of a dichloride salt, where the organic part has two positive charges distributed along its chain.

In each of the crystals, the PQ salts were crystallized into distinct crystalline systems and space groups. The anhydrous salt was crystallized in the orthorhombic system, for which the space group is P*nma*; the structure of the dihydrate salt is found in the triclinic system and space group P $\bar{1}$; and, finally, the trihydrate form of the salt is found in the monoclinic system and space group $P2_1/c$. PQC-I unit cell volume corresponds to 1575.41 Å^3 and 19.9% of this total was calculated as void space (Supplementary Figure S1: Supplementary Material S1). In PQC-II and PQC-III, the unit cell volumes are filled by the chemical entities of the respective salts, in which in the latter, the excess H_2O molecule raises the volume of the former in the proportion of 2.2:1. PQC-I, PQC-II, and PQC-III crystallographic data are shown in Table 1. In Section 3.2, other characteristics inherent to the crystalline structures of these salts will be discussed.

The PQC-II and PQC-III geometric parameters were compared with the PQC-I by the mean absolute deviation percent formula,

$$\mathrm{MADP} = \frac{100}{n}\sum_{i=1}^{n}\left|\frac{\chi_{PQC-X} - \chi_{PQC-I}}{\chi_{PQC-I}}\right|, \quad (4)$$

where χ_{PQC-X} is the geometric parameters of the PQC-II and PQC-III and χ_{PQC-I} is the PQC-I geometric parameters. The graphs in Supplementary Figure S2 (Supplementary Material S1) show the comparison results carried out for the bond length and angle. The presence of water molecules does not significantly alter the BP cation structure. However, in PQC-III, we observed that the bond lengths are more sensitive to H_2O, where the MADP value was 1.801%; in PQC-II,

TABLE 2 Reactivity indices for bipyridylium cation, salt and radical, obtained at M06-2X/6-311++G(d,p) level of theory.

Descriptor	Cation (kcal/mol)	Salt (kcal/mol)	Radical (kcal/mol)
E_{HOMO}	−387.60	−167.31	−286.14
E_{LUMO}/E_{SOMO}[a]	−222.32	−50.51	−198.41*
$\Delta E_{H\text{-}L}$[b]	165.28	116.81	87.73
Ionization Energy (I)	387.60	167.31	286.14
Electronic Affinity (A)	222.32	50.51	198.41
Electronegativity (χ)	304.96	108.91	242.27
Chemical potential (μ)	−304.96	−108.91	−242.27
Chemical hardness (η)	165.28	116.81	87.73
Electrophilicity index (ω)	281.33	50.77	334.52

[a]In radical, E_{SOMO} (SOMO, singly occupied molecular orbital).
[b]ΔEH-L = ELUMO–EHOMO.

the MADP was 1.606%. H_2O molecules were responsible for stretching the C_1–N_1 and C_{12}–N_2 bonds (on average 4.8%) while compressing the C_2–C_3 and C_{10}–C_{11} bonds (on average 2.8%). On the other hand, the angles in PQC-II showed the greatest deviations, so the MADP value obtained was 0.885%, while in PQC-III, the MADP was 0.850%. Among others, the greatest variations occurred in C_5–C_6–N_1 and C_8–C_9–N_2 angles, whose average increase was 2.2%, except in the case of PQC-II, where the increase in the second was only 1.4%.

The BP cation assumes a planar conformation in the crystals. However, in the gas phase and in the presence of Cl^-anions, the calculations showed that its structure undergoes a torsion in the bond that joins the pyridylium portions, so that the planes formed by the aromatic rings meet at 42.5° (Figure 2A). The total energy scan showed that in conformations where the C_3-C_4-C_7-C_8 dihedral angle in the BP cation is 0° or 180°, the system is in the highest energy state (Figure 2B). However, the total energy is lower by rotating the aromatic portions by 40° and 140°.

FMO for the salt and BP cation are shown in Supplementary Figure S3. The respective HOMO and LUMO energies, as well as the energy gap ($\Delta E_{H\text{-}L}$), are shown in Table 2. According to Pearson's principle, the FMO energy values indicated that the BP cation presents an acid character due to its low E_{LUMO} value. On the other hand, because of the presence of Cl^-ions, salt has a markedly more basic character, which is justified by its high E_{HOMO} value. Furthermore, these data indicate that the BP ion is more susceptible to reduction during the weeds' photosynthesis process. The high $\Delta E_{H\text{-}L}$ value for the cation, together with its high oxidation state, indicates a harder structure and, consequently, less polarizability. Chemical hardness

$$\eta = \frac{1}{2}\left(\frac{\partial^2 E}{\partial N^2}\right)_{v(\mathbf{r})} = \frac{I - A}{2}, \tag{5}$$

is an electronic property that measures the resistance to electron cloud deformation under small perturbations during chemical processes. In Eq. 5, E is the energy of the system, N is the number of particles, $v(\mathbf{r})$ is the external potential at point $\mathbf{r}$, $I \cong -E_{HOMO}$ is the ionization potential, and $A \cong -E_{LUMO}$ is the electron affinity. The presence of the chloride anion in the salt reduces the BP cation's $\Delta E_{H\text{-}L}$ value, allowing an electron cloud distortion in the presence of a momentary dipole; that is, the cation becomes more polarizable. In addition, the salt's higher chemical potential allows charge transfer to lower chemical potential systems. Chemical potential

$$\mu = \left(\frac{\partial E}{\partial N}\right)_{v(\mathbf{r})} = -\frac{I + A}{2} = -\chi, \tag{6}$$

is a measure of the charge transfer from a system of greater μ to one of smaller μ, and χ is the electronegativity. These values agree with the PQ redox processes in the chloroplasts, where the plant photosynthetic systems are contained (Photosystem I). In this environment, the electrons produced during the absorption of light energy are captured by the BP cation, resulting in the formation of a free radical. The results of the spin density calculations showed that the unpaired electron in the free radical is in the p orbitals of the N atoms (Figure 3), whose occupation is 0.84e, and the probability in each one is 0.158.

During the process of plant photosynthesis, PQ is reduced to form a stable radical cation. Spin density calculations showed that the unpaired electron could be located equally on both nitrogen atoms of its structure. This cation rapidly reacts with the molecular oxygen present in chloroplasts, forming the superoxide ion from water molecules. From then on, other reactive oxygen species are formed, initiating lipid peroxidation, and culminating in the rupture of cell membranes.

3.2 Supramolecular arrangement description

HS shows that, in the three crystal structures of PQ, the BP cation interacts with the Cl^-ions as well as the water molecules in the hydrated salts at the same sites, as shown by the red circular regions (Figure 4). In these regions, the van der Waals spheres are superimposed, indicating short contacts, forming classical and non-classical H-bonds. The 2D fingerprint plots showed that the H···Cl contacts of the BP cation with the Cl^-anions correspond to 19.2% of the HS in PQC-I, 15.3% in PQC-II and 11.0% in PQC-III. On the other hand, in PQC-III, the H···O interactions account for 9.8% of the HS, whereas in PQC-II, this area is just 5.8%. The topological

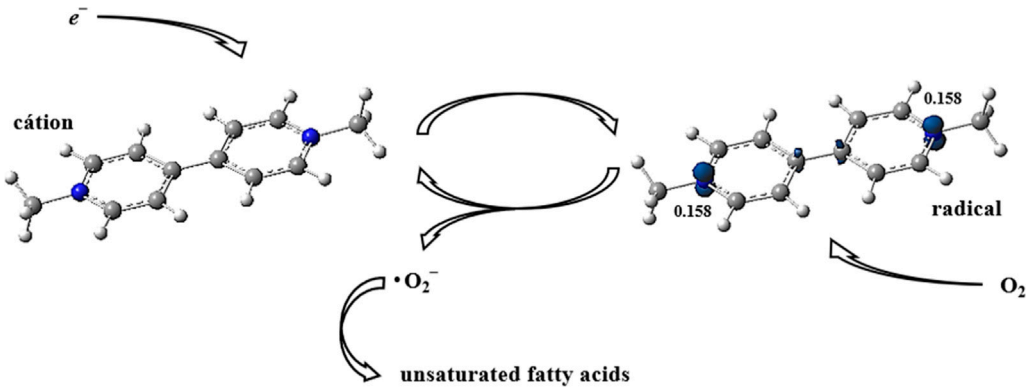

FIGURE 3
Paraquat's mechanism of action on plant chloroplasts. The bipyridylium cation captures the electron produced in photosynthesis and becomes the free radical. The molecular oxygen present in the environment recovers the radical into a cation and transforms it into a superoxide radical, which destroys the unsaturated fatty acids, killing the plant.

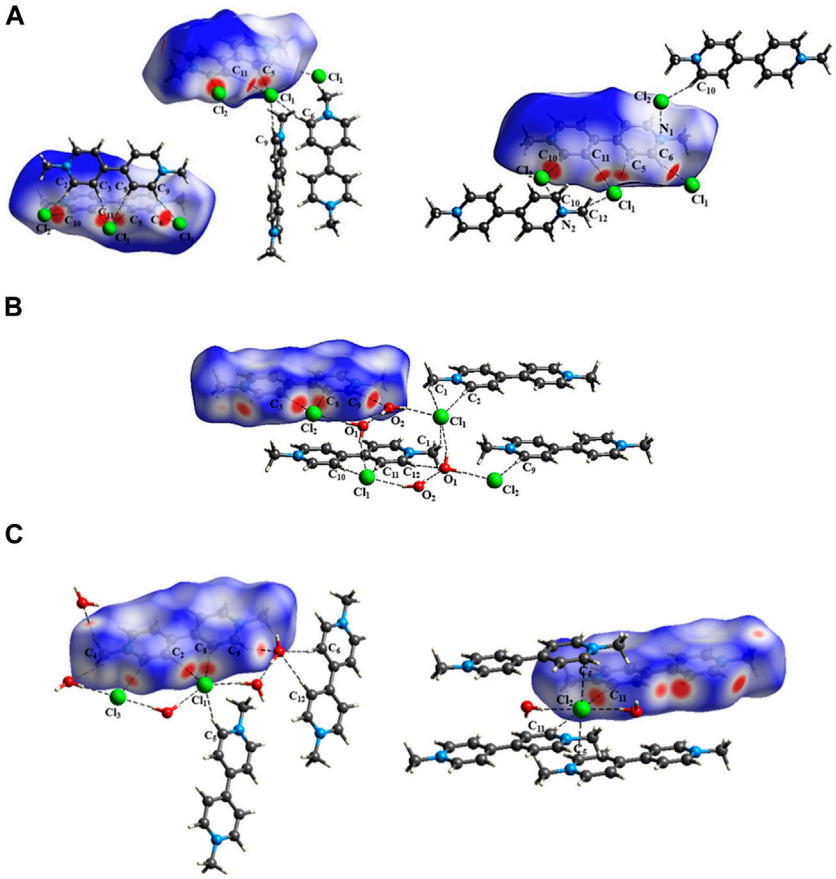

FIGURE 4
Hirshfeld surface d_{norm} showing the intermolecular interactions in **(A)** PQC-I, **(B)** PQC-II, and **(C)** PQC-III supramolecular arrangements of the Paraquat salts. The red spots represent the short contact areas.

parameters provided by QTAIM showed that, in all H···Cl and H···O interactions, the charge densities are very low ($\rho < 0.1$ a.u.) in the respective internuclear regions and $\nabla^2\rho > 0$, indicating that the electrons are depleted in the BCP and configuring *closed-shell* interactions. In these interactions, the nuclear attractors are connected by weak electrostatic interactions. Supplementary Table S1 presents the topological parameters obtained by calculating the structures of the PQ salts. It is notable that the number of interactions increases with the amount of co-crystallized water molecules in the salts.

10.3389/fchem.2023.1267634

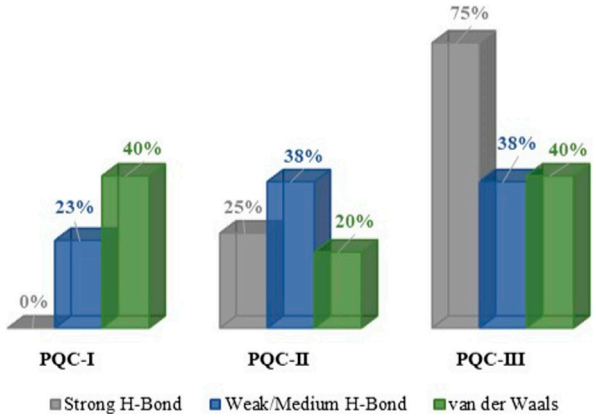

FIGURE 5
Percentage of each type of interaction occurring between the chemical entities in the Paraquat salts.

Furthermore, the total interactions accounted for in three salts (Figure 5) indicated that PQC-III held 75% of the strong H-bond (Hibbert and Emsley, 1990), being attributed to interactions O_3–H···O_1, O_3–H···O_2 and C_1–H···O_2, whose *BE* values are, respectively, −13.60, −17.62, and −13.36 kcal/mol. In PQC-II, the H atom bonded to C_1 does not interact with O atoms. van der Waals interactions occur to a lesser extent in the PQC-II supramolecular arrangement, which is attributed only to C_5–H···Cl_1, where *BE* is −4.39 kcal/mol. However, the C_5–H···Cl_1 interaction also occurs in PQC-I, with *BE* being −6.45 kcal/mol, where, together with the topological parameters, it presents a weak/medium H-bond character. The C_2–H···Cl_x interaction was observed in three crystalline environments. However, the associated energy increases in the order PQC-III < PQC-II < PQC-I, where the data point to a van der Waals interaction character in the trihydrate salt.

It was observed that in the interactions C_8–H···Cl_x the *BE* values are similar in PQC-I and PQC-III (−7.51 and −7.05 kcal/mol). In PQC-I, the charge density in BCP is about 1.08 times greater, and, in addition, the slightly greater angle C_8–H–Cl_x confers a more effective superimposition of the orbitals involved. In PQC-II, although this angle is quite favorable for orbital overlap, the Cl^-ion is stressed in the structure, forming a structure like a pyramid with a "square" base, with the Cl^-anion slightly below the plane of this base. However, the topological parameters indicated that in the three cases, C_8–H–Cl_x is weak/medium H-bond. The C_{10}–H–Cl_x interaction is very weak in PQC-I, showing a van der Waals character.

Finally, while the C_9–H···O_y interaction in PQC-II is a strong H-bond, in PQC-III it is a van der Waals interaction, with the highest *BE* value in its supramolecular arrangement. This effect is because in PQC-III, the water molecule responsible for this interaction is strongly connected to two other water molecules, which in turn are connected to two Cl^-ions, minimizing the contribution of the lone pair from O_3.

3.3 Environmental impact

PQ is usually applied in the post-emergence of weeds in small concentrations (Cui et al., 2019), being absorbed by the foliage and binding strongly to organic and mineral matter, making it biologically inert. For this reason, PQ quickly became a hit on the market, given that the agriculturist could spray the weeds 1 day and sow the crop the next. PQ is poorly translocated within plants due to the rapid desiccation of plant tissues, so tubers and roots are not affected and can grow back. In addition, this herbicide is quickly absorbed by the soil, where the process of sorption is essentially ion exchange, and is deactivated, allowing new crops to be cultivated immediately without risk of phytotoxicity (Weber et al., 1965; Weber and Weed, 1968; Wibawa et al., 2009).

PQ also occurs in non-photosynthetic tissues, such as those of mammals. In these organisms, the compound is reduced through electron transfer in microsomes and mitochondria (Cochemé and Murphy, 2008), the mechanism being like that of photosynthetic systems. PQ is poorly absorbed through intact skin but can penetrate through skin wounds, which is of concern as the compound is a skin irritant (Tabak et al., 1990). Oral exposure is not considered relevant due to its low volatility; however, studies show that inhalation exposure may depend on climatic conditions. Oral exposure can occur through splashing in the mouth during mixing and transport, eating with contaminated hands, blowing on or sucking on spray nozzles, or eating contaminated food.

PQ's toxic effects are observed not only in wildlife [terrestrial insects, birds, mammals, fish, algae, aquatic macrophytes, crustacean larvae, frogs (Eisler, 1990)], domesticated animal [cats, dogs, pigs, sheep, poultry, and geese (van Oers et al., 2005)], and human (Tsai, 2013) populations, but also in ecosystems. These include small lakes (Way et al., 1971) and reservoirs (Brooker and Edwards, 1973) from temperate and tropical regions, the latter including the Cerrado biome. PQ can thus harm non-target organisms (Martins, 2013), thus reducing biodiversity and the ecosystem services related to food security and farming profitability (Dennis et al., 2018). Furthermore, the intoxication of individuals can result in death, depending on ingested PQ concentration and species' sensitivity; among vertebrates, mammals, including humans, are the most sensitive, displaying acute intoxication symptoms at 22–35 mg kg^{-1} body weight (Eisler, 1990; Huang et al., 2019). Intoxication can occur through bioaccumulation, expressed by injuries in the lungs (Tsai, 2013) and kidneys (McGwin and Griffin, 2022), and can contribute to Parkinson's disease in humans (Zhang et al., 2016). However, PQ's toxicity is not experienced only by vertebrates; it interferes with the habitat selection processes of fish (*Oreochromis niloticus* in this case), meaning that suitable habitats for fish with PQ concentrations higher than1.0 mg/L are avoided because of their low habitat quality, leading to the population's decline (Soriwei et al., 2021).

Regarding the Cerrado biome, the contact of PQ with environmental biotic and abiotic components is facilitated by agricultural activity, resulting in low habitat quality and habitat loss when natural areas are converted to agricultural production (Schiesari and Grillitsch, 2011). However, the influence of PQ on the terrestrial environment is limited because of soil adsorption capacity associated with good agricultural practices. It is these practices and conditions that minimize the risk of causing pollution while protecting natural resources and allowing economically viable agriculture to continue, and in these conditions the use of PQ is not detrimental to soil-dwelling flora and fauna in the long term (Roberts et al., 2002). A similar situation is observed in the aquatic environment, where PQ's availability is restricted because it is adsorbed by particles and sediment (Thi Hue et al., 2018). This situation

seems to explain the few studies conducted to assess its toxicity for the environment in the Cerrado biome [influence of PQ on mortality of tadpoles (Lajmanovich et al., 1998) and native bees (Peruzzolo et al., 2021) and potential danger for freshwater species (Lundberg, 2021)], although the Brazilian Cerrado has been intensively used for agricultural purposes since the 1980s, involving the use of herbicides such as PQ. However, the current use of good agricultural practices in the Cerrado, such as no-till agriculture, seems not to prevent the environmental impacts of herbicides like PQ, because it aims for the expansion and profitability of large-scale farming based on input-intensive practices instead of sustainable agriculture processes (Ofstehage and Nehring, 2021).

4 Conclusion

The structure and reactivity of the BP cation, isolated and in PQ salts, were investigated, and theoretical data were used to understand the cation's tendency for electronic capture during photosynthetic processes in chloroplasts, resulting in the formation of a stable free radical. The supramolecular arrangement structures of PQ salts showed that co-crystallization of H_2O molecules leads to an increase in the number of strong interactions in the respective crystals. The Cerrado biome in central Brazil is composed of unique vegetation types that are a large source of bioactive compounds and provide great opportunities for sustainable agricultural practices. This biome has been used for agricultural purposes for some time, involving the use of the herbicide PQ until 2020, and the few studies conducted in Cerrado areas confirm its toxicity for the environment. While no decision has been made on the future use of PQ in Brazil, environmental studies based on legislation and physicochemical properties are essential to analyzing it within agriculture's dynamic sector.

Data availability statement

The original contributions presented in the study are included in the article/Supplementary Materials, further inquiries can be directed to the corresponding authors.

Author contributions

AA: Conceptualization, Formal Analysis, Investigation, Methodology, Project administration, Resources, Supervision, Validation, Visualization, Writing–original draft, Writing–review and editing. LC: Resources, Writing–original draft, Writing–review and editing. IB: Investigation, Resources, Writing–original draft, Writing–review and editing. GA: Conceptualization, Data curation, Formal Analysis, Investigation, Supervision, Visualization, Writing–review and editing. FT-G: Formal Analysis, Investigation, Methodology, Resources, Validation, Visualization, Writing–original draft, Writing–review and editing. SD: Formal Analysis, Investigation, Methodology, Resources, Validation, Visualization, Writing–original draft, Writing–review and editing. HN: Conceptualization, Data curation, Formal Analysis, Methodology, Project administration, Resources, Supervision, Validation, Visualization, Writing–review and editing.

Funding

The author(s) declare that no financial support was received for the research, authorship, and/or publication of this article.

Acknowledgments

The authors are grateful to Coordenação de Aperfeiçoamento de Pessoal de Nível Superior, Fundação de Amparo à Pesquisa do Estado de Goiás, and Conselho Nacional de Desenvolvimento Científico e Tecnológico for financial support. The authors are also grateful to the High-Performance Computing Center of the Universidade Estadual de Goiás (UEG).

Conflict of interest

The authors declare that the research was conducted in the absence of any commercial or financial relationships that could be construed as a potential conflict of interest.

Publisher's note

Supplementary material

The Supplementary Material for this article can be found online at: https://www.frontiersin.org/articles/10.3389/fchem.2023.1267634/full#supplementary-material

References

Aekrathok, P., Songsri, P., Jongrungklang, N., and Gonkhamdee, S. (2021). Efficacy of post-emergence herbicides against important weeds of sugarcane in north-east Thailand. *Agronomy* 11, 429. doi:10.3390/agronomy11030429

Argay, G., and Kálmán, A. (1995). Crystal structure of 1,1′-dimethyl-4,4′-bipyridinium dichloride trihydrate, $C_{12}H_{14}N_2Cl_2(H_2O)_3$. *Z. Krist. Cryst. Mater.* 210, 455–456. doi:10.1524/zkri.1995.210.6.455

Bader, R. F. W. (1994). *Atoms in molecules - a quantum theory*. Ontario: Clarendon Press Publication.

Bader, R. F. W. (1985). Atoms in molecules. *Acc. Chem. Res.* 18, 9–15. doi:10.1021/ar00109a003

Brazil (2020). *Resolução de Diretoria Colegiada - RDC N° 428 de 7 de Outubro de 2020.*

Brian, R. C., Homer, R. F., Stubbs, J., and Jones, R. L. (1958). A new herbicide: 1 : 1′-Ethylene-2 : 2′-Dipyridylium dibromide. *Nat. Lond.* 181, 446–447. doi:10.1038/181446a0

Brooker, M. P., and Edwards, R. W. (1973). Effects of the herbicide paraquat on the ecology of a reservoir. *Freshw. Biol.* 3, 157–175. doi:10.1111/j.1365-2427.1973.tb00070.x

Brown, R., Clapp, M., Dyson, J., Scott, D., Wheals, I., and Wilks, M. (2004). Paraquat in perspective. *Outlooks Pest Manag.* 15, 259–267. doi:10.1564/15dec09

Cabette, A., Freitas, H., and Aranha, A. (2020). Brasil é 2º maior comprador de agrotóxicos proibidos na Europa, que importa alimentos produzidos com estes químicos. *Repórter Brasil/Agência Pública*. Available at: https://reporterbrasil.org.br/2020/09/%EF%BB%BFbrasil-e-2o-maior-comprador-de-agrotoxicos-proibidos-na-europa-que-importa-alimentos-produzidos-com-estes-quimicos/(Accessed April 29, 2023).

Cambridge Crystallographic Data Centre, Inc (2023). CCDC- the Cambridge crystallographic data Centre. *Camb. Struct. Database (CSD)*. Available at: https://www.ccdc.cam.ac.uk/(Accessed August 15, 2023).

Carroll, M. T., and Bader, R. F. W. (1988). An analysis of the hydrogen bond in BASE-HF complexes using the theory of atoms in molecules. *Mol. Phys.* 65, 695–722. doi:10.1080/00268978800101351

Cochemé, H. M., and Murphy, M. P. (2008). Complex I is the major site of mitochondrial superoxide production by paraquat. *J. Biol. Chem.* 283, 1786–1798. doi:10.1074/jbc.M708597200

Cousson, A., Bachet, B., Kokel, B., and Hubert-Habart, M. (1993). Structure of N,N'-dimethyl-4,4'-bipyridylium dichloride dihydrate. *Acta Crystallogr. C* 49, 942–943. doi:10.1107/S0108270191015019

Cui, F., Brosché, M., Shapiguzov, A., He, X. Q., Vainonen, J. P., Leppälä, J., et al. (2019). Interaction of methyl viologen-induced chloroplast and mitochondrial signalling in Arabidopsis. *Free Radic. Biol. Med.* 134, 555–566. doi:10.1016/j.freeradbiomed.2019.02.006

da Silva, D. R. O., de Aguiar, A. C. M., Basso, C. J., and Muraro, D. S. (2021). Application time affects synthetic auxins herbicides in tank-mixture with paraquat on hairy fleabane control. *Rev. Ceres* 68, 194–200. doi:10.1590/0034-737X202168030005

de Queiroz, V. T., Azevedo, M. M., da Silva Quadros, I. P., Costa, A. V., do Amaral, A. A., dos Santos, G. M. A. D. A., et al. (2018). Environmental risk assessment for sustainable pesticide use in coffee production. *J. Contam. Hydrol.* 219, 18–27. doi:10.1016/j.jconhyd.2018.08.008

Dennis, P. G., Kukulies, T., Forstner, C., Orton, T. G., and Pattison, A. B. (2018). The effects of glyphosate, glufosinate, paraquat and paraquat-diquat on soil microbial activity and bacterial, archaeal and nematode diversity. *Sci. Rep.* 8, 2119. doi:10.1038/s41598-018-20589-6

Dodge, A. D. (1982). The role of light and oxygen in the action of photosynthetic inhibitor herbicides. *ACS Symp. Ser.* 181, 57–77. doi:10.1021/bk-1982-0181.ch004

Dutra e Silva, S. (2023). "Ecological ideas and historical construction of the Brazilian Cerrado," in *Ore – Latin American history* (Oxford University Press).

Eisler, R. (1990). *Paraquat hazards to fish, wildlife, and invertebrates: A synoptic review*. Washington, DC: Biological Report - US Fish and Wildlife Service.

Emamian, S., Lu, T., Kruse, H., and Emamian, H. (2019). Exploring nature and predicting strength of hydrogen bonds: A correlation analysis between atoms-in-molecules descriptors, binding energies, and energy components of symmetry-adapted perturbation theory. *J. Comput. Chem.* 40, 2868–2881. doi:10.1002/jcc.26068

Ferreira, A. C. B., Bogiani, J. C., Sofiatti, V., and da Silva Filho, J. L. (2018). Chemical control of stalk regrowth in glyphosate-resistant transgenic cotton. *Rev. Bras. Eng. Agric. Ambient.* 22, 530–534. doi:10.1590/1807-1929/agriambi.v22n8p530-534

Frisch, M. J., Trucks, G. W., Schlegel, H. B., Scuseria, G. E., Robb, M. A., Cheeseman, J. R., et al. (2016). *Gaussian 16, revision C.01*.

Fukushima, T., Tanaka, K., Lim, H., and Moriyama, M. (2002). Mechanism of cytotoxicity of paraquat. *Environ. Health Prev. Med.* 7, 89–94. doi:10.1265/ehpm.2002.89

Glaeser, B. (2010). *The green revolution revisited: Critique and alternatives*. 1st ed. London: Taylor and Francis.

Hibbert, F., and Emsley, J. (1990). "Hydrogen bonding and chemical reactivity," in *Advances in physical organic Chemistry*. Editor D. Bethell (Liverpool, 255–379. doi:10.1016/S0065-3160(08)60047-7

Hohenberg, P., and Kohn, W. (1964). Inhomogeneous electron gas. *Phys. Rev.* 136, B864–B871. doi:10.1103/physrev.136.b864

Huang, Y., Zhan, H., Bhatt, P., and Chen, S. (2019). Paraquat degradation from contaminated environments: Current achievements and perspectives. *Front. Microbiol.* 10, 1754. doi:10.3389/fmicb.2019.01754

Jacob, C. R., and Reiher, M. (2012). Spin in density-functional theory. *Int. J. Quantum Chem.* 112, 3661–3684. doi:10.1002/qua.24309

Kohn, W., and Sham, L. J. (1965). Self-consistent equations including exchange and correlation effects. *Phys. Rev.* 140, A1133–A1138. doi:10.1103/physrev.140.a1133

Lajmanovich, R. C., Izaguirre, M. F., and Casco, V. H. (1998). Paraquat tolerance and alteration of internal gill structure of Scinax nasica tadpoles (Anura: Hylidae). *Arch. Environ. Contam. Toxicol.* 34, 364–369. doi:10.1007/s002449900331

Lima, T. L., Nicoletti, M. A., Munhoz, C., Ramos De Abreu, G., Zaccarelli Magalhães, J., Ricci, E. L., et al. (2018). Determination of paraquat in several commercially available types of rice. *Food Nutr. Sci.* 9, 1368–1375. doi:10.4236/fns.2018.912098

Lu, T., and Chen, F. (2012). Multiwfn: A multifunctional wavefunction analyzer. *J. Comput. Chem.* 33, 580–592. doi:10.1002/jcc.22885

Lundberg, A. (2021). *Regional differences in pesticide use and footprints of Brazilian soybeans*. Gothenburg, Sweden: Chalmers - University of Technology.

Macrae, C. F., Bruno, I. J., Chisholm, J. A., Edgington, P. R., McCabe, P., Pidcock, E., et al. (2008). Mercury CSD 2.0 - new features for the visualization and investigation of crystal structures. *J. Appl. Crystallogr.* 41, 466–470. doi:10.1107/S0021889807067908

Macrae, C. F., Edgington, P. R., McCabe, P., Pidcock, E., Shields, G. P., Taylor, R., et al. (2006). Mercury: Visualization and analysis of crystal structures. *J. Appl. Crystallogr.* 39, 453–457. doi:10.1107/S002188980600731X

Martins, T. (2013). Herbicida paraquat: Conceitos, modo de ação e doenças relacionadas. *Semina Ciências Biológicas Saúde* 34, 175. doi:10.5433/1679-0367.2013v34n2p175

Matta, C. F., and Bader, R. F. W. (2003). Atoms-in-molecules study of the genetically encoded amino acids. III. Bond and atomic properties and their correlations with experiment including mutation-induced changes in protein stability and genetic coding. *Proteins Struct. Funct. Genet.* 52, 360–399. doi:10.1002/prot.10414

McGwin, G., and Griffin, R. L. (2022). An ecological study regarding the association between paraquat exposure and end stage renal disease. *Environ. Health* 21, 127. doi:10.1186/s12940-022-00946-9

Michaelis, L., and EdgarHill, S. (1933). Potentiometric studies on semiquinones. *J. Am. Chem. Soc.* 55, 1481–1494. doi:10.1021/ja01331a027

Ofstehage, A., and Nehring, R. (2021). No-till agriculture and the deception of sustainability in Brazil. *Int. J. Agric. Sustain.* 19, 335–348. doi:10.1080/14735903.2021.1910419

Oliveira, P. S., and Marquis, R. J. (2002). in *The cerrados of Brazil*. Editors P. Oliveira and R. Marquis (New York Chichester: Columbia University Press). doi:10.7312/oliv12042

Overhauser, A. W. (1962). Spin density waves in an electron gas. *Phys. Rev.* 128, 1437–1452. doi:10.1103/PhysRev.128.1437

Paumgartten, F. J. R. (2020). Pesticides and public health in Brazil. *Curr. Opin. Toxicol.* 22, 7–11. doi:10.1016/j.cotox.2020.01.003

Peruzzolo, M. C., Grange, L., and Ronqui, L. (2021). Mortalidade de abelhas sem ferrão Scaptotrigona bipunctata sob os efeitos dos herbicidas paraquat e diquat. *Arq. Ciências Veterinárias Zool. UNIPAR* 24. doi:10.25110/arqvet.v24i1cont.2021.8408

Rial-Otero, R., Cancho-Grande, B., Perez-Lamela, C., Simal-Gandara, J., and Arias-Estevez, M. (2006). Simultaneous determination of the herbicides diquat and paraquat in water. *J. Chromatogr. Sci.* 44, 539–542. doi:10.1093/chromsci/44.9.539

Roberts, T. R., Dyson, J. S., and Lane, M. C. G. (2002). Deactivation of the biological activity of paraquat in the soil environment: A review of long-term environmental fate. *J. Agric. Food Chem.* 50, 3623–3631. doi:10.1021/jf011323x

Rocha, C. B., de Majo, C., and Dutra e Silva, S. (2022a). A geo-historical analysis of expanding soybean frontiers in the Brazilian Cerrado. *Hist. Ambient. Latinoam. Caribeña (HALAC) Rev. Solcha* 12, 217–252. doi:10.32991/2237-2717.2022v12i2.p217-252

Rocha, C. B., Nehring, R., and Silva, S. D. E. (2022b). Soy without borders: The transnational dynamics of commodity frontiers in south America (1971-2019). *Glob. Environ.* 15, 423–455. doi:10.3197/ge.2022.150301

Russell, J. H., and Wallwork, S. C. (1972). The crystal structures of the dichloride and isomorphous dibromide and diiodide of the N,N'-dimethyl-4,4'-bipyridylium ion. *Acta Crystallogr. B* 28, 1527–1533. doi:10.1107/S0567740872004534

Santos, M. S. F., Schaule, G., Alves, A., and Madeira, L. M. (2013). Adsorption of paraquat herbicide on deposits from drinking water networks. *Chem. Eng. J.* 229, 324–333. doi:10.1016/j.cej.2013.06.008

Schiesari, L., and Grillitsch, B. (2011). Pesticides meet megadiversity in the expansion of biofuel crops. *Front. Ecol. Environ.* 9, 215–221. doi:10.1890/090139

Shoham, J. (2013). Quantifying the economic and environmental benefits of paraquat. *Outlooks Pest. Manag.* 24, 64–69. doi:10.1564/v24_apr_05

Soriwei, E. T., Umeokeke, H. C., Amaeze, H. N., Ogunfeitimi, O. O., and Labinjo, A. S. (2021). Dichlorvos and paraquat induced spatial avoidance response: A more realistic determinant of population decline of *Oreochromis niloticus*. *Ecotoxicol. Environ. Contam.* 16, 27–34. doi:10.5132/eec.2021.01.04

Spackman, M. A., and Jayatilaka, D. (2009). Hirshfeld surface analysis. *Cryst. Eng. Comm.* 11, 19–32. doi:10.1039/b818330a

Spackman, M. A., and McKinnon, J. J. (2002). Fingerprinting intermolecular interactions in molecular crystals. *Cryst. Eng. Comm.* 4, 378–392. doi:10.1039/b203191b

Tabak, A., Taitelman, U., and Hoffer, E. (1990). Percutaneous permeability to paraqut: *In vitro* experiments with human skin. *J. Toxicol. Cutan. Ocul. Toxicol.* 9, 301–311. doi:10.3109/15569529009036334

Thi Hue, N., Nguyen, T. P. M., Nam, H., and Hoang Tung, N. (2018). Paraquat in surface water of some streams in mai chau province, the northern vietnam: Concentrations, profiles, and human risk assessments. *J. Chem.* 2018, 1–8. doi:10.1155/2018/8521012

Tsai, W.-T. (2013). A review on environmental exposure and health risks of herbicide paraquat. *Toxicol. Environ. Chem.* 95, 197–206. doi:10.1080/02772248.2012.761999

Turner, M., McKinnon, J., Wolff, S., Grimwood, D., Spackman, P., Jayatilaka, D., et al. (2017). *CrystalExplorer17*.

van Oers, L., Tamis, W., Koning, A., and Snoo, G. (2005). *Review of incidents with wildlife related to paraquat*. Leiden, Netherlands: CML Library.

Veríssimo, G., Moreira, J. C., and Meyer, A. (2018). Paraquat contamination in surface waters of a rural stream in the mountain region in the state of Rio De Janeiro southeastern Brazil. *J. Environ. Toxicol. Stud.* 2. doi:10.16966/2576-6430.111

Way, J. M., Newman, J. F., Moore, N. W., and Knaggs, F. W. (1971). Some ecological effects of the use of paraquat for the control of weeds in small lakes. *J. Appl. Ecol.* 8, 509. doi:10.2307/2402887

Weber, J. B., Perry, P. W., and Upchurch, R. P. (1965). The influence of temperature and time on the adsorption of paraquat, diquat, 2,4-D and prometone by clays, charcoal, and an anion-exchange resin. *Soil Sci. Soc. Am. J.* 29, 678–688. doi:10.2136/sssaj1965.03615995002900060026x

Weber, J. B., and Weed, S. B. (1968). Adsorption and desorption of diquat, paraquat, and prometone by montmorillonitic and kaolinitic clay minerals. *Soil Sci. Soc. Am. J.* 32, 485–487. doi:10.2136/sssaj1968.03615995003200040020x

Wibawa, W., Mohamad, R. B., Puteh, A. B., Omar, D., Juraimi, A. S., and Abdullah, S. A. (2009). Residual phytotoxicity effects of paraquat, glyphosate and glufosinate-ammonium herbicides in soils from field-treated plots. *Int. J. Agric. Biol.* 11, 214–216.

Zhang, G., and Musgrave, C. B. (2007). Comparison of DFT methods for molecular orbital eigenvalue calculations. *J. Phys. Chem. A* 111, 1554–1561. doi:10.1021/jp061633o

Zhang, X., Thompson, M., and Xu, Y. (2016). Multifactorial theory applied to the neurotoxicity of paraquat and paraquat-induced mechanisms of developing Parkinson's disease. *Lab. Investig.* 96, 496–507. doi:10.1038/labinvest.2015.161

Zhao, Y., and Truhlar, D. G. (2008). The M06 suite of density functionals for main group thermochemistry, thermochemical kinetics, noncovalent interactions, excited states, and transition elements: Two new functionals and systematic testing of four M06-class functionals and 12 other functionals. *Theor. Chem. Acc.* 120, 215–241. doi:10.1007/s00214-007-0310-x